

# Low-Latency Network-Adaptive Error Control for Interactive Streaming

Silas L. Fong, Salma Emara, Baochun Li, Ashish Khisti, Wai-Tian Tan, Xiaoqing Zhu, and John Apostolopoulos

**Abstract**—We introduce a novel network-adaptive algorithm that is suitable for alleviating network packet losses for low-latency interactive communications between a source and a destination. Our network-adaptive algorithm estimates in real time the best parameters of a recently proposed streaming code that uses forward error correction (FEC) to correct both arbitrary and burst losses, which cause crackling noise and undesirable jitters respectively in audio. In particular, the destination estimates appropriate coding parameters based on its observed packet loss pattern and sends them back to the source for updating the underlying code. In addition, a new explicit construction of practical low-latency streaming codes that achieve the optimal tradeoff between the capability of correcting arbitrary losses and the capability of correcting burst losses is provided. Simulation evaluations based on statistical losses and real-world packet loss traces reveal the following: (i) Our proposed network-adaptive algorithm combined with our optimal streaming codes can achieve significantly higher performance compared to uncoded and non-adaptive FEC schemes over UDP (User Datagram Protocol); (ii) Our explicit streaming codes can significantly outperform traditional MDS (maximum-distance separable) streaming schemes when they are used along with our network-adaptive algorithm.

## I. INTRODUCTION

REAL-time interactive streaming is an essential component for many low-latency applications over the Internet including high-definition video conferencing, augmented/virtual reality, and online gaming. In particular, low-latency video conferencing has been a cornerstone for communication and collaboration for individuals and enterprises. At the core of these important applications is the need to reliably deliver packets with low latency. Given that the Internet is a packet-switched network where reliable packet delivery is not guaranteed, the need for effective methods to protect live video communications over the Internet has never been greater.

### A. Forward Error Correction for Real-Time Streaming

Packet erasure (loss) at the network layer for an end-to-end communication over the Internet is inevitable. Two main approaches have been implemented at the transport layer to control end-to-end error introduced by the network layer:

This paper will be presented at 27th ACM International Conference on Multimedia, Nice, France, 2019.

S. L. Fong is with Qualcomm Flarion Technologies, NJ 08807, USA (E-mail: [silas.fong@ieee.org](mailto:silas.fong@ieee.org)).

S. Emara, B. Li and A. Khisti are with the Department of Electrical and Computer Engineering, University of Toronto, Toronto, ON M5S 3G4, Canada (E-mails: [salma@ece.utoronto.ca](mailto:salma@ece.utoronto.ca), [bli@ece.utoronto.edu](mailto:bli@ece.utoronto.edu), [akhisti@ece.utoronto.ca](mailto:akhisti@ece.utoronto.ca)).

W.-T. Tan, X. Zhu and J. Apostolopoulos are with Cisco Systems, San José, CA 95134, USA.

Automatic repeat request (ARQ) and forward error correction (FEC). Both ARQ and FEC can alleviate the damages of packet losses that may be caused by unreliable wireless links or congestion at network bottlenecks. However, ARQ schemes are not suitable for real-time streaming applications that involve arbitrary global users because each retransmission will incur an extra round-trip delay which may be intolerable. Specifically, correcting an erasure using ARQ results in a 3-way delay (forward + backward + forward), and this aggregate (3-way) delay including transmission, propagation and processing delays is required to be lower than 150 ms for interactive applications such as voice and video according to the International Telecommunication Union (ITU) [1,2]. This aggregate delay makes ARQ impractical for communication between two distant global users with aggregate delay larger than 150 ms due to the following argument as presented in [3]: The minimum possible aggregate delay between two diametrically opposite points on the earth's circumference is at least 200 ms even if the signals travel at the speed of light. Consequently, any ARQ scheme implemented at the transport layer including the commonly used transport-layer protocol TCP (Transmission Control Protocol) is not suitable for low-latency interactive streaming among global users.

On the contrary, FEC schemes are amenable to low-latency communications among global users because no retransmission is required. Instead of using retransmissions to achieve high reliability, FEC schemes increase the correlation among the transmitted symbols by adding redundant information. Then, any erased packet may be reconstructed by the redundant information in the subsequent surviving packets. Low-density parity-check (LDPC) [4,5] codes and digital fountain codes [6,7] are two traditional FEC schemes that are currently used in the DVB-S2 [8] and DVB-IPTV [9] standards for non-interactive streaming applications. These codes operate over long block lengths, typically a few thousand symbols, and are thus suitable for applications in which the delay constraints are not stringent. However, LDPC and fountain codes are not suitable for interactive streaming applications where short block lengths (e.g., a few hundred symbols) are required due to the stringent delay constraints. On the other hand, low-latency FEC schemes that operate over short block lengths have been proposed to improve interactive communication [10]–[13]. Indeed, the use of FEC schemes for protecting voice streams against packet erasures has largely attributed to the success of Skype [14], and an adaptive hybrid NACK/FEC has been used in WebRTC to obtain a better trade-off between temporal quality, spatial video quality and end-to-end delay [13].

### B. Main Contributions

Recently, several systematic studies have been carried out to characterize the fundamental limits of streaming codes (i.e., low-latency FEC schemes) that correct burst and arbitrary (isolated) erasures [15]–[17], where the former is usually due to network congestion and the latter can be caused by unreliable wireless links. In particular, the authors in [16,17] have provided a high-complexity construction of a class of FEC streaming codes that possess the following two properties:

- (a) Both arbitrary and burst erasures can be corrected, which cause crackling noise and undesirable jitters/pauses respectively for audio.
- (b) Under a given maximum delay constraint, the optimal tradeoff between the capability of correcting arbitrary erasures and the capability of correcting burst erasures can be achieved.

Therefore, we are motivated to design a real-time error control scheme based on low-complexity FEC streaming codes that satisfy Properties (a) and (b) and implement the design in real-world networks. Our real-time error control design consists of the following properties:

- (i) A new explicit construction of low-latency streaming codes that achieve the optimal tradeoff between the capability of correcting arbitrary erasures and the capability of correcting burst erasures under a given maximum delay constraint.
- (ii) In order to take varying network conditions into account, we also design a network-adaptive algorithm that updates the parameters of our constructed low-latency streaming codes in real time as follows: The destination estimates appropriate coding parameters based on its observed erasure pattern and then the estimated parameters are fed back to the source for updating the code.

In addition, we conduct simulations and real-world experiments to demonstrate the performance of our network-adaptive FEC streaming scheme. Our simulation and experimental results reveal that our network-adaptive scheme achieves significantly higher reliability compared to uncoded and non-adaptive FEC schemes over UDP (User Datagram Protocol). Note that the maximum delay constraint that appeared in Property (b) and Property (i) is a suitable delay metric for interactive communication because any packet recovered beyond a certain threshold must be discarded in order to avoid undesirable pauses (recall the 150 ms threshold recommended by ITU for interactive voice and video). On the contrary, the average delay metric is more relevant for non-interactive streaming applications such as video streaming, which has been used in [18]–[21] to study the tradeoff between throughput and average delay for non-interactive streaming where no packet is ever discarded.

### C. Paper Outline

The remainder of the paper is organized as follows. Section II reviews how streaming codes correct packet erasures. Section III formulates optimal streaming codes that correct both burst and arbitrary erasures. Section IV presents our explicit construction for optimal streaming codes over GF(256).

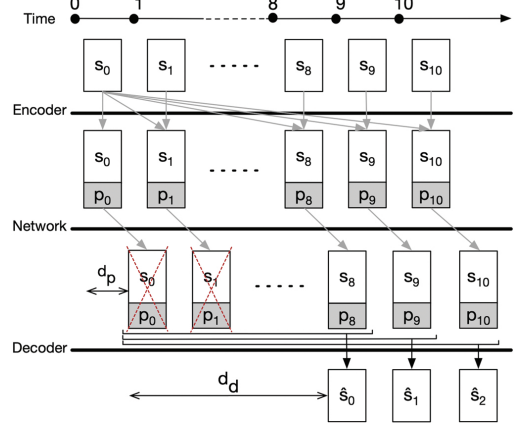


Fig. 1: A general FEC framework



Fig. 2: Packet drops marked by dark squares

Section V proposes a heuristic network-adaptive algorithm that estimates the best optimal streaming codes adaptively based on real-time channel information. Section VI suggests the prototype of a network-adaptive FEC streaming scheme that uses our explicit streaming codes in Section IV and our network-adaptive algorithm in Section V as building blocks. Section VII presents both simulation and experimental results that show the following: Our network-adaptive scheme suggested in Section VI can outperform traditional schemes not only in simulation environments, but also in real-world wireless networks. Section VIII concludes this paper and lists possible directions for future work.

This work enriches our preliminary results in [22] by adding the following new materials:

- (a) Reproducible simulation results to be presented in Section VII-C.
- (b) Experimental results expressed in terms of comprehensive metrics including frame loss rate (FLR), coding rate and PESQ score [23], which will be presented in Section VII-D.
- (c) A more in-depth comparison between using traditional FEC streaming codes and using our explicit streaming codes along with our network-adaptive algorithm will be presented in Section VII-C3 and Section VII-D3, which identifies the scenarios that we can benefit from using our explicit streaming codes compared with traditional FEC streaming codes.

## II. CONCEPT OF FEC STREAMING CODES

We first present a general framework of FEC streaming code as illustrated in Figure 1. The source periodically generates a sequence of multimedia frames. Each multimedia frame is concatenated with a parity frame, and they are encapsulated in a network packet which travels to the destination with a propagation delay  $d_p$ . The network packets can be dropped by

the network in an arbitrary manner due to unreliable (wireless) links or in a bursty manner due to network congestion, which are illustrated in Figure 2 respectively. The destination aims to recover the multimedia frames sequentially subject to a decoding delay constraint  $d_d$ , where lost multimedia frames can be recovered with the help of subsequent parity frames. For example, if packets 0 and 1 are dropped as illustrated in Figure 1, then the parity frames in packets 2 to 8 may help recover frame 0 with decoding delay of 8 frames, and the parity frames in packets 2 to 9 may help recover frame 1 with the same decoding delay. If we follow existing FEC technologies (e.g., webRTC [13] and Skype [14]) and choose the parity frames based on coding over the past multimedia frames using maximum-distance separable (MDS) codes, the resulting FEC streaming code is optimal for correcting arbitrary losses subject to the decoding delay  $d_d$ . However, in order to achieve the optimal tradeoff between the capability of correcting arbitrary losses and the capability of correcting burst losses subject to a decoding delay constraint, we have to carefully choose the parity frames. The existence of such optimal parity frames has been recently proved in [16,17]. More precisely, given a decoding delay constraint of  $T$  frames and any coding parameters  $(B, N)$  such that  $T \geq B \geq N \geq 1$ , there exists an optimal choice for the parity frames which leads to a capacity-achieving streaming code that can correct length- $B$  burst erasures and  $N$  arbitrary erasures.

### III. FORMULATION OF STREAMING CODES

#### A. Notation

The sets of natural numbers and non-negative integers are denoted by  $\mathbb{N}$  and  $\mathbb{Z}_+$  respectively. A finite field is denoted by  $\mathbb{F}$ . The set of  $k$ -dimensional row vectors over  $\mathbb{F}$  is denoted by  $\mathbb{F}^k$ . A row vector in  $\mathbb{F}^k$  is denoted by  $\mathbf{a} \triangleq [a_0 \ a_1 \ \dots \ a_{k-1}]$ . The  $k$ -dimensional identity matrix is denoted by  $\mathbf{I}_k$  and the  $L \times B$  all-zero matrix is denoted by  $\mathbf{0}^{L \times B}$ . An  $L \times B$  parity matrix of a systematic MDS  $(L+B, L)$ -code is denoted by  $\mathbf{V}^{L \times B}$ , which possesses the property that any  $L$  columns of  $[\mathbf{I}_L \ \mathbf{V}^{L \times B}] \in \mathbb{F}^{L \times (L+B)}$  are independent. It is well known [24] that a systematic MDS  $(L+B, L)$ -code always exists as long as  $|\mathbb{F}| \geq L+B$ .

#### B. Definitions and Optimality of Streaming Codes

The following three definitions are standard [15]–[17].

**Definition 1:** An  $(n, k, T)_{\mathbb{F}}$ -streaming code consists of:

- 1) A sequence of messages  $\{\mathbf{s}_i\}_{i=0}^{\infty}$  where  $\mathbf{s}_i \in \mathbb{F}^k$ .
- 2) An encoder  $f_i : \mathbb{F}^k \times \dots \times \mathbb{F}^k \rightarrow \mathbb{F}^n$  for each  $i \in \mathbb{Z}_+$ , where  $f_i$  is used by the source at channel use  $i$  to encode the source symbols according to

$$\mathbf{x}_i = f_i(\mathbf{s}_0, \mathbf{s}_1, \dots, \mathbf{s}_i).$$

- 3) A decoder  $\varphi_{i+T} : \mathbb{F}^n \cup \{\ast\} \times \dots \times \mathbb{F}^n \cup \{\ast\} \rightarrow \mathbb{F}^k$  for each  $i \in \mathbb{Z}_+$ , where  $\ast$  denotes the erasure symbol and  $\varphi_{i+T}$  is used by the destination at channel use  $i+T$  to estimate  $\mathbf{s}_i$  according to

$$\hat{\mathbf{s}}_i = \varphi_{i+T}(\mathbf{y}_0, \mathbf{y}_1, \dots, \mathbf{y}_{i+T}).$$

**Definition 2:** An  $(n, k, T)_{\mathbb{F}}$ -streaming code is said to *correct any  $(B, N)$ -erasure sequence* if  $\hat{\mathbf{s}}_i = \mathbf{s}_i$  holds for all  $i \in \mathbb{Z}_+$  for the following sliding-window channel: In any sliding window  $\{i, i+1, \dots, i+T\}$  of size  $T+1$  starting at channel use  $i \in \mathbb{Z}_+$ , either a burst erasure of length at most  $B$  or multiple erasures of count at most  $N$  are introduced.

**Definition 3:** The  $(T, B, N)$ -capacity is the maximum rate  $k/n$  achievable by  $(n, k, T)_{\mathbb{F}}$ -streaming codes that correct all  $(B, N)$ -erasure sequences, which is formally defined as

$$\sup \left\{ \frac{k}{n} \mid \text{There exists an } (n, k, T)_{\mathbb{F}}\text{-streaming code that corrects all } (B, N)\text{-erasure sequences for some } \mathbb{F} \right\}.$$

**Theorem 1** ([16,17]): Define

$$C(T, B, N) \triangleq \frac{T - N + 1}{T - N + B + 1}. \quad (1)$$

For any  $T \geq B \geq N \geq 1$ , the  $(T, B, N)$ -capacity equals  $C(T, B, N)$  as defined in (1).

Theorem 1 motivates the definition of optimal codes below.

**Definition 4:** For any  $T \geq B \geq N \geq 1$ , an  $(n, k, T)_{\mathbb{F}}$ -code that corrects any  $(B, N)$ -erasure sequence is said to be *optimal* if  $\frac{k}{n} = C(T, B, N)$ .

### IV. EXPLICIT CONSTRUCTION OF OPTIMAL STREAMING CODES OVER GF(256)

Although the existence of optimal streaming codes has been proved in [16,17], no explicit construction over practical field size was given. Motivated by the fact that finite fields with characteristic 2 allow very efficient computation, we provide the first explicit construction of optimal streaming codes over GF(256) when  $T \leq 11$ . Readers who are uninterested in the explicit construction may skip the remaining part of this section and take the following result for granted:

“Let  $\mathbb{F} = \text{GF}(256)$ . For any  $T \geq B \geq N \geq 1$ , an  $(n, k, T)_{\mathbb{F}}$ -code that corrects any  $(B, N)$ -erasure can be efficiently generated.”

The explicit construction leverages a standard periodic interleaving approach which constructs streaming codes based on block codes as defined below.

**Definition 5:** An  $(n, k, T)_{\mathbb{F}}$ -block code consists of:

- 1) A sequence of  $k$  symbols  $\{s[i]\}_{i=0}^{k-1}$  where  $s[i] \in \mathbb{F}$ .
- 2) A generator matrix  $\mathbf{G} \in \mathbb{F}^{k \times n}$ . The *source codeword* is generated as

$$[x[0] \ x[1] \ \dots \ x[n-1]] = [s[0] \ s[1] \ \dots \ s[k-1]] \ \mathbf{G}.$$

- 3) A decoder  $\varphi_{i+T} : \mathbb{F}^n \cup \{\ast\} \times \dots \times \mathbb{F}^n \cup \{\ast\} \rightarrow \mathbb{F}$  for each  $i \in \{0, 1, \dots, k-1\}$ , where  $\ast$  is the erasure symbol and  $\varphi_{i+T}$  is used by the destination at channel use  $\min\{i+T, n-1\}$  to estimate  $s[i]$  according to

$$\hat{s}[i] = \varphi_{i+T}(y[0], \dots, y[\min\{i+T, n\}]).$$

**Definition 6:** An  $(n, k, T)_{\mathbb{F}}$ -block code is said to *correct any  $(B, N)$ -erasure sequence* if  $\hat{s}_i = s_i$  holds for all  $i \in \mathbb{Z}_+$  as long as either a burst erasure of length at most  $B$  or multiple erasures of count at most  $N$  occur in every sliding window of size  $T+1$ . The block code is said to be *optimal* if  $\frac{k}{n} = C(T, B, N)$ .

We will leverage the following lemma to construct optimal streaming codes based on optimal block codes. The lemma is a direct consequence of [16, Lemma 1] with the identification  $W = T + 1$ . The proof is standard and is based on periodic interleaving (cf. [25] and [15, Sec. IV-A]).

*Lemma 1* ([16, Lemma 1]): Given an  $(n, k, T)_{\mathbb{F}}$ -block code which corrects any  $(B, N)$ -erasure sequence, we can construct an  $(n, k, T)_{\mathbb{F}}$ -streaming code which corrects any  $(B, N)$ -erasure sequence.

Due to Lemma 1, Definition 4 and Definition 6, the search for explicit construction of optimal streaming codes over GF(256) reduces to the search for explicit construction of optimal block codes over GF(256).

#### A. Structures of Parity Matrices of Optimal Block Codes

The following two lemmas state specific structures of the parity matrices of optimal codes. The lemmas are expressed with the help of the following definition of an  $m$ -row  $N$ -diagonal matrix:

$$\mathbf{D}_N^{m \times (N+m)} \triangleq \begin{bmatrix} d_0^{(0)} & \cdots & d_{N-1}^{(0)} & 0 & \cdots & \cdots & 0 \\ 0 & d_0^{(1)} & \cdots & d_{N-1}^{(1)} & 0 & \cdots & 0 \\ \vdots & \ddots & \ddots & \ddots & \ddots & \ddots & \vdots \\ 0 & \cdots & 0 & d_0^{(m-1)} & \cdots & d_{N-1}^{(m-1)} & 0 \end{bmatrix}$$

where  $\{d_{\ell}^{(i)} \mid 0 \leq i \leq m-1, 0 \leq \ell \leq N-1\}$  assume arbitrary values.

*Lemma 2* ([16, Lemmas 2, 3 and 4]): Fix any  $T \geq B \geq N \geq 1$  and let  $k \triangleq T - N + 1$  and  $n \triangleq k + B$ . If  $k \geq B$  (i.e.,  $k/n \geq 1/2$ ), there exists a  $\mathbf{P}$  having the form

$$\begin{bmatrix} \mathbf{D}_N^{(B-N) \times B} \\ \mathbf{0}^{N \times (B-N)} \\ \mathbf{V}^{(k-B) \times B} \end{bmatrix} \quad (2)$$

such that  $\mathbf{G} = [\mathbf{I}_k \ \mathbf{P}]$  is the generator matrix of an  $(n, k, T)$ -code that corrects any  $(B, N)$ -erasure sequences, where  $\mathbf{D}_N^{m \times (N+m)}$  is an  $m$ -row  $N$ -diagonal matrix,  $\mathbf{P}_{\text{right}}$  is an  $N \times N$  matrix, and  $\mathbf{V}^{(k-B) \times B}$  is a  $(k-B) \times B$  parity matrix of a systematic MDS code. On the other hand, if  $k < B$  (i.e.,  $k/n < 1/2$ ), there exists a  $\mathbf{P}$  having the form

$$\begin{bmatrix} \mathbf{P}_{\text{left}} & \mathbf{D}_{k-B+N}^{(B-N) \times k} \\ \mathbf{V}_{\text{left}}^{(k-B+N) \times (B-k)} & \mathbf{0} \quad \mathbf{V}_{\text{right}}^{(k-B+N) \times (k-B+N)} \end{bmatrix} \quad (3)$$

such that  $\mathbf{G} = [\mathbf{I}_k \ \mathbf{P}]$  is the generator matrix of an  $(n, k, T)$ -code that corrects any  $(B, N)$ -erasure sequence, where  $\mathbf{D}_{k-B+N}^{(B-N) \times k}$  is a  $(B-N)$ -row  $(k-B+N)$ -diagonal matrix,  $[\mathbf{V}_{\text{left}}^{(k-B+N) \times (B-k)} \ \mathbf{V}_{\text{right}}^{(k-B+N) \times (k-B+N)}]$  constitutes the  $(k-B+N) \times N$  parity matrix of a systematic MDS code,  $\mathbf{P}_{\text{left}}$  is a  $(B-N) \times (B-k)$  matrix, and  $\mathbf{0}$  is the  $(k-B+N) \times (B-N)$  zero matrix.

The structures of  $\mathbf{P}$  in (2) and (3) motivate us to construct optimal codes over GF(256) as described below.

#### B. Deterministic Construction of Parity Matrices of Optimal Codes over GF(256)

Assume  $\mathbb{F} = \text{GF}(256)$  in the rest of the paper. Suppose we are given a  $k \times B$  matrix  $\mathbf{V}^{k \times B}$  where  $k \geq 1$  and  $B \geq 1$ , and let  $n \triangleq k + B$ . Then, we construct a parity matrix  $\mathbf{P} \in \mathbb{F}^{k \times B}$  as follows.

- If  $k \geq B$ , construct  $\mathbf{P}$  by replacing every non-zero  $(i, j)^{\text{th}}$  element of  $\mathbf{P}$  in (2) with the  $(i, j)^{\text{th}}$  element in  $\mathbf{V}^{k \times B}$ .
- If  $k < B$ , construct  $\mathbf{P}$  by replacing every non-zero  $(i, j)^{\text{th}}$  element of  $\mathbf{P}$  in (3) with the  $(i, j)^{\text{th}}$  element in  $\mathbf{V}^{k \times B}$ .

Let  $\mathcal{C}(\mathbf{V}^{k \times B})$  denote the  $(n, k, T)_{\mathbb{F}}$ -block code with generator matrix  $\mathbf{G}$  as constructed above. If  $\mathcal{C}(\mathbf{V}^{k \times B})$  corrects any  $(B, N)$ -erasure sequence and  $k = T - N + 1$ , then  $\mathcal{C}(\mathbf{V}^{k \times B})$  is optimal by Definition 4. In search of a suitable  $\mathbf{V}^{k \times B}$ , we define  $\mathbf{V}_{\text{Cauchy}}^{(T-N+1) \times B} = [v_{ij}^{\text{Cauchy}}]_{\substack{0 \leq i \leq T-N \\ 0 \leq j \leq B-1}}$  to be a  $(T-N+1) \times B$  Cauchy matrix over GF(256) where  $v_{ij}^{\text{Cauchy}} \triangleq (i+j+k)^{-1}$ . Similarly, define  $\mathbf{V}_{\text{Vand}}^{(T-N+1) \times B} = [v_{ij}^{\text{Vand}}]_{\substack{0 \leq i \leq T-N \\ 0 \leq j \leq B-1}}$  to be a  $(T-N+1) \times B$  Vandermonde matrix over GF(256) where  $v_{ij}^{\text{Vand}} \triangleq 2^{i \times j}$ . Using computer search, we obtain the following.

*Proposition 3*: Let  $\mathbb{F} = \text{GF}(256)$ . For any  $1 \leq N \leq B \leq T \leq 11$ , the  $(n, k, T)_{\mathbb{F}}$ -block code  $\mathcal{C}(\mathbf{V}_{\text{Cauchy}}^{(T-N+1) \times B})$  corrects any  $(B, N)$ -erasure if  $(T, B, N) \notin \{(10, 8, 4), (11, 5, 4)\}$ . In addition,  $\mathcal{C}(\mathbf{V}_{\text{Vand}}^{(T-N+1) \times B})$  corrects any  $(B, N)$ -erasure if  $(T, B, N) \in \{(10, 8, 4), (11, 5, 4)\}$ .

In view of Proposition 3, define for any  $1 \leq N \leq B \leq T \leq 11$  the parity matrix of an optimal  $(n, k, T)_{\mathbb{F}}$ -block code as

$$\mathbf{V}_{\text{optimal}}^{(T-N+1) \times B} \triangleq \begin{cases} \mathbf{V}_{\text{Cauchy}}^{(T-N+1) \times B} & \text{if } (T, B, N) \notin \{(10, 8, 4), (11, 5, 4)\}, \\ \mathbf{V}_{\text{Vand}}^{(T-N+1) \times B} & \text{otherwise.} \end{cases}$$

We will use  $\mathbf{V}_{\text{optimal}}^{(T-N+1) \times B}$  to construct optimal streaming codes as described in the next subsection.

#### C. Deterministic Construction of Optimal Streaming Codes

Using Proposition 3 and the definition of  $\mathbf{V}_{\text{optimal}}^{(T-N+1) \times B}$ , we conclude that  $\mathcal{C}(\mathbf{V}_{\text{optimal}}^{(T-N+1) \times B})$  is an optimal block code. In addition, we can construct an optimal streaming code by periodically interleaving  $n$  copies of  $\mathcal{C}(\mathbf{V}_{\text{optimal}}^{(T-N+1) \times B})$  as illustrated below (cf. Lemma 1).

*Example 1*: Suppose we are given a  $(6, 3, 5)_{\mathbb{F}}$ -block code that corrects any  $(3, 2)$ -erasure sequence with generator matrix

$$\mathbf{G} = \begin{bmatrix} 1 & 0 & 0 & 1 & 1 & 0 \\ 0 & 1 & 0 & 0 & 1 & 1 \\ 0 & 0 & 1 & 0 & 1 & 2 \end{bmatrix}.$$

The block code is optimal by Definition 4. Suppose we have a streaming message  $\{\mathbf{s}_i\}_{i \in \mathbb{Z}_+}$  where  $\mathbf{s}_i = [s_i[0] \ s_i[1] \ s_i[2]] \in \mathbb{F}^3$ . From channel use  $i-2$  to  $i+5$ , the symbols yielded by the  $(6, 3, 5)_{\mathbb{F}}$ -code constructed by periodically interleaving the  $(6, 3, 5)_{\mathbb{F}}$ -block code according Lemma 1 are shown in Table I. The symbols in Table I which are highlighted in the same color diagonally (in direction  $\searrow$ ) are encoded using the

Symbol \ Channel use	$i - 2$	$i - 1$	$i$	$i + 1$	$i + 2$	$i + 3$	$i + 4$	$i + 5$
0	$s_{i-2}[0]$	$s_{i-1}[0]$	$s_i[0]$	$s_{i+1}[0]$	$s_{i+2}[0]$	$s_{i+3}[0]$	$s_{i+4}[0]$	$s_{i+5}[0]$
1	$s_{i-2}[1]$	$s_{i-1}[1]$	$s_i[1]$	$s_{i+1}[1]$	$s_{i+2}[1]$	$s_{i+3}[1]$	$s_{i+4}[1]$	$s_{i+5}[1]$
2	$s_{i-2}[2]$	$s_{i-1}[2]$	$s_i[2]$	$s_{i+1}[2]$	$s_{i+2}[2]$	$s_{i+3}[2]$	$s_{i+4}[2]$	$s_{i+5}[2]$
3	..	..	..	$s_{i-2}[0]$	$s_{i-1}[0]$	$s_i[0]$	..	..
4	..	..	..	..	$s_{i-2}[0]$ + $s_{i-1}[1]$ + $s_i[2]$	$s_{i-1}[0]$ + $s_i[1]$ + $s_{i+1}[2]$	$s_i[0]$ + $s_{i+1}[1]$ + $s_{i+2}[2]$	..
5	..	..	..	..	..	$s_{i-1}[1]$ + $2s_i[2]$	$s_i[1]$ + $2s_{i+1}[2]$	$s_{i+1}[1]$ + $2s_{i+2}[2]$

TABLE I: Symbols yielded by a  $(6, 3, 5)_{\mathbb{F}}$ -code through interleaving a  $(6, 3, 5)_{\mathbb{F}}$ -block code.

same  $(6, 3, 5)_{\mathbb{F}}$ -block code. Given the fact that the  $(6, 3, 5)_{\mathbb{F}}$ -block code corrects any  $(3, 2)$ -erasure sequence, we can see from Table I that  $\mathbf{s}_i = [s_i[0] \ s_i[1] \ s_i[2]]$  can be perfectly recovered by channel use  $i + 5$  as long as a burst erasure of length no longer than 3 or no more than 2 arbitrary erasures occur in every sliding window of size 6.

By periodically interleaving  $n$  copies of  $\mathcal{C}(\mathbf{V}_{\text{optimal}}^{(T-N+1) \times B})$ , we can construct an  $(n, k, T)$ -code with  $k = T - N + 1$  and  $n = k + B$ , which is optimal if  $T \leq 11$  by Proposition 3. For any  $1 \leq N \leq B \leq T \leq 11$ , we let  $\mathcal{C}_{T, B, N}$  denote the optimal  $(n, k, T)$ -code that is constructed by interleaving  $n$  copies of  $\mathcal{C}(\mathbf{V}_{\text{optimal}}^{(T-N+1) \times B})$ . The optimal streaming codes  $\mathcal{C}_{T, B, N}$  are the building blocks for the network-adaptive streaming scheme described in the next section.

## V. NETWORK-ADAPTIVE ALGORITHM

### A. A Conservative Algorithm that Estimates Channel Parameters $B$ and $N$ in $L$ Channel Uses

We first present a conservative algorithm illustrated by Algorithm 1 that estimates conservative coding parameters  $B$  and  $N$  in  $L$  channel uses. Before the algorithm tracks any packet erasures, the decoding delay denoted by  $T$  and the duration of the algorithm denoted by  $L$  are fixed, and the initial estimates for  $B$  and  $N$ , denoted by  $\hat{B}_{-1}$  and  $\hat{N}_{-1}$  respectively, are both set to 0. In other words, the channel is assumed to be initially ideal which introduces no erasure. In addition, the variable  $N_{\max}$  which keeps track of the maximum number of arbitrary erasures is set to 0.

Every packet transmitted at channel use  $i \in \mathbb{Z}_+$  is assumed to either reach the destination in the same channel use or be erased. In practice, packets that are either dropped in a network or received in the wrong order are erased. For example, if packets are received in the order  $0, 1, 3, 2, 4$ , packet 2 is considered to be erased. For every non-erased packet received at channel use  $i \in \mathbb{Z}_+$ , the algorithm first deduces the erasure pattern  $e_{\mathcal{W}} \triangleq (e_{j-T}, e_{j-T+1}, \dots, e_j) \in \{0, 1\}^{T+1}$  for each sliding window  $\mathcal{W} = \{j - T, j - T + 1, \dots, j\}$  of size  $T + 1$  such that  $j \leq i$ , where an element of  $e_{\mathcal{W}}$  equals 1 if and only if the corresponding packet is erased. Let  $\text{wt}(e_{\mathcal{W}}) \triangleq \sum_{\ell \in \mathcal{W}} e_{\ell}$  and

$$\text{span}(e_{\mathcal{W}}) \triangleq \begin{cases} 0 & \text{if } \text{wt}(e_{\mathcal{W}}) = 0, \\ p_{\text{last}} - p_{\text{first}} + 1 & \text{otherwise,} \end{cases}$$

be the *weight* and *span* of  $e_{\mathcal{W}}$  respectively, where  $p_{\text{first}}$  and  $p_{\text{last}}$  denote respectively the channel use indices of the first and

### Algorithm 1: Estimating conservative $B$ and $N$

---

**Result:**  $\hat{B}_i$  and  $\hat{N}_i$  are generated at the destination for every packet  $i$  where  $0 \leq i \leq L - 1$ . All correctible length- $(T + 1)$  erasure patterns that occur by channel use  $i$  can be perfectly recovered by any code that corrects all  $(\hat{B}_i, \hat{N}_i)$ -erasures.

**Inputs :**  $T, L$  and  $e^L$  denoting decoding delay, duration, and length- $L$  erasure pattern respectively.

**Outputs:**  $\hat{B}_i$  and  $\hat{N}_i$  for every packet  $i$ .

```

1 previous_seq_# ← -1
2  $(\hat{B}_{-1}, \hat{N}_{-1}, N_{\max}) \leftarrow (0, 0, 0)$ 
3 for  $i \leftarrow 0$  to  $L - 1$  do // packets 0 to  $L - 1$  sent
4   if  $e_i = 0$  then // packet  $i$  not erased
5     current_seq_# ←  $i$ 
6     for  $j \leftarrow \text{previous\_seq\_#} + 1$  to  $\text{current\_seq\_#}$  do
7        $\mathcal{W} \leftarrow \{j - T, j - T + 1, \dots, j\}$ 
8        $\hat{B}_j \leftarrow \max\{\text{span}(e_{\mathcal{W}}), \hat{B}_{j-1}\}$ 
9        $\hat{N}_j \leftarrow \max\{\text{wt}(e_{\mathcal{W}}), \hat{N}_{j-1}\}$ 
10       $N_{\max} \leftarrow \max\{\text{wt}(e_{\mathcal{W}}), N_{\max}\}$ 
11      if  $\hat{N}_j = 0$  or  $\hat{N}_j = T + 1$  then // trivial
12         $(\hat{B}_j, \hat{N}_j) \leftarrow (\hat{B}_{j-1}, \hat{N}_{j-1})$ 
13      else // compute 3 hypothetic rates
14         $R_B \leftarrow \begin{cases} 0 & \text{if } \bar{B} = T + 1, \\ C(T, \bar{B}_j, \max\{\hat{N}_{j-1}, 1\}) & \text{if } \bar{B} < T + 1 \end{cases}$ 
15         $R_N \leftarrow C(T, \max\{\hat{B}_{j-1}, \bar{N}_j\}, \bar{N}_j)$ 
16         $R_{\text{MDS}} \leftarrow C(T, N_{\max}, N_{\max})$ 
17        switch  $\max\{R_B, R_N, R_{\text{MDS}}\}$  do
18          case  $R_B$  do //  $R_B$  largest
19             $(\hat{B}_j, \hat{N}_j) \leftarrow (\bar{B}_j, \max\{\hat{N}_{j-1}, 1\})$ 
20            break
21          case  $R_N$  do //  $R_N$  largest
22             $(\hat{B}_j, \hat{N}_j) \leftarrow (\max\{\hat{B}_{j-1}, \bar{N}_j\}, \bar{N}_j)$ 
23            break
24          case  $R_{\text{MDS}}$  do //  $R_{\text{MDS}}$  largest
25             $(\hat{B}_j, \hat{N}_j) \leftarrow (N_{\max}, N_{\max})$ 
26        end
27      end
28    end
29    previous_seq_# ←  $\text{current\_seq\_#}$ 
30  end
31 end

```

---

last non-zero elements in  $e_{\mathcal{W}}$ . Intuitively speaking,  $\text{span}(e_{\mathcal{W}})$  is the minimum length over all intervals that contain the support of  $e_{\mathcal{W}}$ . For each deduced erasure pattern  $e_{\mathcal{W}} = (e_{j-T}, e_{j-T+1}, \dots, e_j)$ , the algorithm first calculates  $\text{wt}(e_{\mathcal{W}})$  and  $\text{span}(e_{\mathcal{W}})$ , and then assign the values to  $(\bar{B}_j, \bar{N}_j, N_{\max})$  according to

$$\begin{aligned}\bar{B}_j &:= \max\{\text{span}(e_{\mathcal{W}}), \hat{B}_{j-1}\}, \\ \bar{N}_j &:= \max\{\text{wt}(e_{\mathcal{W}}), \hat{N}_{j-1}\},\end{aligned}$$

and

$$N_{\max} := \max\{\text{wt}(e_{\mathcal{W}}), N_{\max}\}.$$

Then one of the following updates will occur:

- (i)  $\hat{B}_j$  will be assigned the value  $\bar{B}_j$ .
- (ii)  $\hat{N}_j$  will be assigned the value  $\bar{N}_j$ .
- (iii) Both  $\hat{B}_j$  and  $\hat{N}_j$  will be assigned the value  $N_{\max}$ .

More specifically, the estimates  $\hat{B}_j$  and  $\hat{N}_j$  will be output according to the following three mutually exclusive cases:

**Case  $\bar{N}_j = 0$ :** In this case,

$$\bar{B}_j = \bar{N}_j = \text{wt}(e_{\mathcal{W}}) = \text{span}(e_{\mathcal{W}}) = \hat{N}_{j-1} = \hat{B}_{j-1} = 0,$$

which implies that no erasure has yet occurred upon the receipt of packet  $j$ . Then, Algorithm 1 sets  $\hat{N}_j = \hat{B}_j = 0$ , meaning that the estimates for  $N$  and  $B$  remain to be zeros.

**Case  $\bar{N}_j = T + 1$ :** In this case, all the elements of  $e_{\mathcal{W}}$  equal one, meaning that all the packets in the window  $\{j - T, j - T + 1, \dots, j\}$  are erased, which implies that no  $(n, k, T)_{\mathbb{F}}$ -code can correct  $e_{\mathcal{W}}$ . Therefore, Algorithm 1 sets  $\hat{N}_j = \hat{N}_{j-1}$  and  $\hat{B}_j = \hat{B}_{j-1}$ , meaning that the estimates for  $N$  and  $B$  remain unchanged.

**Case  $0 < \bar{N}_j \neq T + 1$ :** In this case, every length- $(T + 1)$  erasure pattern  $\varepsilon^{T+1}$  that has occurred up to channel use  $j$  can be classified into the following two types, with the terminology that  $\varepsilon^{T+1}$  is a  $(B, N)$ -erasure sequence if either  $\text{span}(e_{\mathcal{W}}) \leq B$  or  $\text{wt}(e_{\mathcal{W}}) \leq N$  holds:

- (i)  $\varepsilon^{T+1}$  consists of all ones, hence it is uncorrectable;
- (ii)  $\varepsilon^{T+1}$  is simultaneously a  $(\bar{B}_j, \max\{\hat{N}_{j-1}, 1\})$ -erasure sequence, a  $(\max\{\hat{B}_{j-1}, \bar{N}_j\}, \bar{N}_j)$ -erasure sequence, and a  $(N_{\max}, N_{\max})$ -erasure sequence.

Note that by construction, every length- $(T + 1)$  erasure pattern up to channel use  $j - 1$  can be classified into either Type (i) or is an  $(\hat{B}_{j-1}, \hat{N}_{j-1})$ -erasure sequence. Therefore, Algorithm 1 calculates the best estimates for  $\hat{B}_j$  and  $\hat{N}_j$  so that the following two conditions hold:

- (I) Every length- $(T + 1)$  erasure pattern up to channel use  $j$  can be classified into either Type (i) or is a  $(\hat{B}_j, \hat{N}_j)$ -erasure sequence.
- (II) The loss in the maximum achievable rate induced by updating the estimates from  $(\hat{B}_{j-1}, \hat{N}_{j-1})$  to  $(\hat{B}_j, \hat{N}_j)$  is minimized.

The presence of Condition (II) is essential because it guarantees that the algorithm cannot output the trivial estimates  $\hat{B}_j = \hat{N}_j = T$  that lead to the lowest rate  $C(T, T, T) = \frac{1}{T+1}$ .

In order to calculate the best estimates for  $\hat{B}_j$  and  $\hat{N}_j$  so that Conditions (I) and (II) hold, Algorithm 1 computes three hypothetic rates based on the  $(T, B, N)$ -capacity as follows:

$$\begin{aligned}R_B &:= \begin{cases} 0 & \text{if } \bar{B}_j = T + 1, \\ C(T, \bar{B}_j, \max\{\hat{N}_{j-1}, 1\}) & \text{if } \bar{B}_j < T + 1, \end{cases} \\ R_N &:= C(T, \max\{\bar{B}_{j-1}, \bar{N}_j\}, \bar{N}_j)\end{aligned}$$

and

$$R_{\text{MDS}} := C(T, N_{\max}, N_{\max})$$

respectively, where  $R_B$  denotes the hypothetic maximum achievable rate if  $\hat{B}_j$  is assigned the value  $\bar{B}_j$  followed by  $\hat{N}_j$  being assigned the value  $\max\{\hat{N}_{j-1}, 1\}$  (note that any  $(\hat{B}_j, \hat{N}_{j-1})$ -erasure sequence is also a  $(\hat{B}_j, \max\{\hat{N}_{j-1}, 1\})$ -erasure sequence),  $R_N$  denotes the hypothetic maximum achievable rate if  $\hat{N}_j$  is assigned the value  $\bar{N}_j$  followed by  $\hat{B}_j$  being assigned the value  $\max\{\hat{B}_{j-1}, \hat{N}_j\}$  (note that any  $(\hat{B}_{j-1}, \hat{N}_j)$ -erasure sequence is also a  $(\max\{\hat{B}_{j-1}, \hat{N}_j\}, \hat{N}_j)$ -erasure sequence), and  $R_{\text{MDS}}$  denotes the hypothetic maximum rate if both  $\hat{B}_j$  and  $\hat{N}_j$  are assigned the same value  $N_{\max}$ . Algorithm 1 sets  $(\hat{B}_j, \hat{N}_j)$  as shown at the end of the pseudocode so that the resultant maximum achievable rate  $C(T, \hat{B}_j, \hat{N}_j)$  equals  $\max\{R_B, R_N, R_{\text{MDS}}\}$ .

Combining the above three cases, we conclude that for all  $0 \leq i \leq L - 1$ , Algorithm 1 generates estimates  $(\hat{B}_i, \hat{N}_i)$  such that Conditions (I) and (II) hold.

### B. Interleaved Conservative Algorithm Based on Algorithm 1

Algorithm 1 provides conservative estimates for  $B$  and  $N$  in the sense that the algorithm yields a code that perfectly corrects all length- $(T + 1)$  correctible erasure sequences that have been observed. An obvious drawback of Algorithm 1 is that the sequence of recommended coding rates is monotonically decreasing over time. Therefore, we propose the following *network-adaptive algorithm* based on interleaving Algorithm 1 as follows: At each channel use  $\ell = 0, L, 2L, \dots$ , an instance of Algorithm 1 denoted by  $\mathcal{A}_\ell$  is initiated. Each  $\mathcal{A}_\ell$  lasts for  $2L$  channel uses, and let  $(\hat{B}_j^{(\ell)}, \hat{N}_j^{(\ell)})$  denote the corresponding estimates generated at channel use  $j$ . Then at each channel use  $j$ , the network-adaptive algorithm outputs the estimate  $(\hat{B}_j^{(\ell)}, \hat{N}_j^{(\ell)})$  provided by  $\mathcal{A}_\ell$  at channel use  $j$  where  $\ell$  is the unique integer that satisfies  $\ell + L \leq j < j + 2\ell$ . In other words, each interleaved Algorithm 1 will run for  $2L$  channel uses where the first  $L$  estimates are ignored by the algorithm and the last  $L$  estimates are output by the network-adaptive algorithm. Due to our construction, the coding rate generated by our network-adaptive algorithm is not monotonically decreasing over time. Particularly, if there are no erasures for consecutive  $2L$  channel uses, the next estimates of  $(B, N)$  would be  $(0, 0)$ .

### VI. NETWORK-ADAPTIVE STREAMING SCHEME

Based on the estimates  $\{(\hat{B}_j, \hat{N}_j)\}_{j \in \mathbb{Z}_+}$  suggested by the network-adaptive algorithm as described in Section V-B (which could be computed at the destination and then fed back to the source), the source adjusts the streaming encoder accordingly so that more erasure patterns can be corrected at the cost of a small rate loss.

### A. Code Transition

Initially starting from channel use 0, the network-adaptive algorithm outputs  $(\hat{B}_0, \hat{N}_0) = (0, 0)$  and the source will use the trivial rate-one encoder so that the transmitted codeword is identical to the generated message. The source continues to use the trivial rate-one encoder until the algorithm updates the estimates for  $B$  and  $N$  to positive values.

Whenever the algorithm provides new estimates for  $(B, N)$  at channel use  $j$  denoted by  $(\hat{B}_j, \hat{N}_j)$ , the source will switch to the new encoder associated with the code  $\mathcal{C}_{T, \hat{B}_j, \hat{N}_j}$  (defined at the end of Section IV). In order to ensure a smooth transition from using an old encoder with parameters  $(B_{\text{old}}, N_{\text{old}})$  to using a new encoder with parameters  $(B_{\text{new}}, N_{\text{new}}) \neq (B_{\text{old}}, N_{\text{old}})$ , the source has to ensure that every transmitted packet is protected by either the old or new encoder. The smooth transition is carried out as described below.

Suppose the source wants to use a new encoder associated with  $\mathcal{C}_{T, B_{\text{new}}, N_{\text{new}}}$  starting from channel use  $i$ , it will use both the old and new encoders to encode the same message into old and new codewords from channel use  $i$  to channel use  $i+T$ . As a result, the messages generated before channel use  $i+T$  are protected by the old codewords in  $\mathcal{C}_{T, B_{\text{old}}, N_{\text{old}}}$ , while the messages generated from channel use  $i+T$  till the next transition will be protected by the new codewords in  $\mathcal{C}_{T, B_{\text{new}}, N_{\text{new}}}$ . During the next transition, the new encoder will be replaced by another encoder and treated as an old encoder, and the transition procedure repeats.

Since every message is protected by either an old encoder with parameters  $(B_{\text{old}}, N_{\text{old}})$  or a new encoder with parameters  $(B_{\text{new}}, N_{\text{new}})$  during the transition, any  $(B_{\text{old}}, N_{\text{old}})$ -erasure sequence of length- $(T+1)$  that occurs before the transition can be corrected by the old encoder and any  $(B_{\text{new}}, N_{\text{new}})$ -erasure sequence of length- $(T+1)$  that occurs during and after the transition can be corrected by the new encoder.

### B. Prototype

The prototype of our proposed network-adaptive streaming scheme is illustrated in Figure 3, which is explained as follows. The parameter estimator uses the network-adaptive algorithm to generate the estimates  $(\hat{B}_i, \hat{N}_i)$  for each  $i \in \mathbb{Z}_+$ . At each channel use  $i$ , an FEC message is generated which consists of a data buffer, an integer specifying the size of the buffer, a sequence number and the latest available estimates  $(\hat{B}, \hat{N})$  fed back from the destination. The FEC message is then encoded into an FEC codeword and transmitted through the erasure channel. Each FEC codeword consists of a codeword buffer, an integer specifying the size of the codeword buffer, the sequence number originated from the corresponding FEC message, and the coding parameters  $(\hat{B}, \hat{N})$ . For every codeword received at channel use  $i$ , the destination decodes all the messages generated before channel use  $i-T$  that have not been decoded yet, where the appropriate decoder can be chosen by the destination based on the coding parameters contained in all the received codewords up to channel use  $i$ . Therefore, every received codeword may result in more than one decoded message. For every reconstructed FEC message,

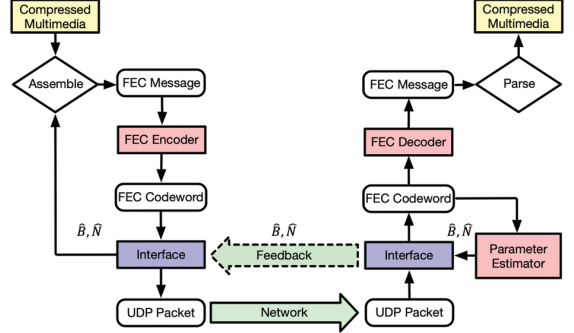


Fig. 3: Prototype of network-adaptive streaming scheme

the corresponding data buffer, the size of the buffer and the sequence number are extracted for further processing.

## VII. SIMULATION AND EXPERIMENTAL RESULTS

In this section, we first design an implementation of our proposed network-adaptive streaming scheme. Next, we present simulation results obtained from a statistical erasure channel which show that our proposed network-adaptive streaming scheme outperforms uncoded and non-adaptive schemes. Finally, we conduct real-world experiments and use the corresponding packet loss traces to demonstrate the performance gain of our network-adaptive streaming scheme over non-adaptive ones.

### A. Implementation of Network-Adaptive Streaming Scheme

In order to explore the potential of our proposed network-adaptive streaming scheme described in Section VI, we implement the proposed scheme for low-latency communication between a source and a destination and present simulation and experimental results that compare our streaming codes with non-adaptive streaming strategies.

Suppose the source transmits a stream of compressed multimedia frames to the destination over the Internet. Each compressed multimedia frame could be generated from raw data by using a standard video codec or voice codec. Next, the compressed frame together with the estimated coding parameters received from the feedback channel is encapsulated in an FEC message. The FEC message is further encoded into an FEC codeword to be encapsulated in a network packet, which is then forwarded to the destination. Every network packet is either received by the intended destination or dropped (erased). At the destination side, every received FEC codeword is extracted from every received network packet and one or more FEC messages are recovered based on the codeword. A recovered compressed multimedia frame is further extracted from every recovered FEC message and then decompressed back to raw data by the video or voice codec.

The two interface modules between the streaming code and the network layer are illustrated in Figure 3. The first module is the interface at the source side that simultaneously encapsulates every FEC codeword into a UDP packet and forwards every estimated parameters received from the feedback channel to the message assembler. The second module is the

interface at the receiver side that simultaneously extracts the codeword buffer in every network packet to form an FEC codeword and forwards every estimated parameters to the feedback channel over UDP.

### B. Parameters and Error Metrics

We compare the frame loss rates (FLRs) achieved by the uncoded scheme and our network-adaptive streaming scheme as described in Section VI. In addition, we illustrate the effectiveness of our proposed network-adaptive algorithm by comparing the FLRs achieved by our adaptive streaming scheme with a delay constraint of  $T$  packets and non-adaptive schemes with fixed coding parameters  $(B, N)$ . To this end, we fix the frame duration and bit rate for the compressed multimedia frame to be 10 ms and 240 kbit/s respectively, which are practical as existing audio codecs typically have frame duration 2.5 – 60 ms and bit rate 6 – 510 kbit/s [26,27]. Consequently, every 300-byte compressed frame is generated every 10 ms. The 10 ms frame duration and the delay constraint  $T$  must be carefully chosen so that the resultant playback delay  $T \times 10$  ms in addition to the propagation delay must be smaller than the 150 ms delay required by ITU for interactive applications [1,2]. For example, if the propagation delay is 100 ms, then the resultant playback delay must be less than  $150 \text{ ms} - 100 \text{ ms} = 50 \text{ ms}$ , which can be achieved by choosing suitable  $T$  and frame duration such that their product is below 50 ms.

For our experimental purpose, we assume the propagation delay is less than 50 ms and choose  $T = 10$  so that the resultant playback delay  $T \times 10$  ms = 100 ms in addition to the propagation delay is below 150 ms. We set  $L = 1000$  for the network-adaptive algorithm described in Section V. In other words, each interleaved Algorithm 1 will run for  $2L \times 10 \times 0.001$  seconds = 20 seconds where the  $L = 1000$  estimates produced in the first 10 seconds are ignored by the algorithm and the next  $L = 1000$  estimates are output by the algorithm.

Let  $M = 360$  be the number of 10-second sessions throughout the transmission, which involves a total of  $L \times M = 360000$  packets lasting for one hour. In each session,  $L = 1000$  packets are transmitted from the source to the destination. For simplicity, let the sequence number of a packet be its channel use index, starting from 0 and ending at  $LM - 1$ . During each session  $m \in \{1, 2, \dots, M\}$ , the source transmits packets with sequence number between  $L(m - 1)$  and  $Lm - 1$ . For each session  $m$ , let  $\varepsilon_m$  denote the corresponding FLR achieved by our network-adaptive streaming scheme. More precisely,  $L(1 - \varepsilon_m)$  is the number of FEC messages with sequence number between  $L(m - 1)$  and  $Lm - 1$  which are perfectly recovered by the destination. We will express in the next two sections our simulation and experimental results respectively in terms of the average FLR defined as  $\frac{1}{M} \sum_{m=1}^M \varepsilon_m$  and the fraction of *low-fidelity* sessions with FLR larger than 10% defined as  $\frac{1}{M} \sum_{m=1}^M \mathbf{1}\{\varepsilon_m > 0.1\}$ .

### C. Simulation Results for a Three-Phase GE Channel

1) *Simulated Frame Loss Rates (FLRs):* We validate the superiority of our network-adaptive streaming scheme as described in Section VII-A to non-adaptive streaming schemes by means of simulating artificial packet erasures according to the Gilbert-Elliott (GE) channel [28,29], which is a well-known statistical channel that is useful for approximating packet losses experienced at the network layer [30,31]. The GE channel is a two-state Markov model which consists of a good state and a bad state. In the good state, each channel packet is lost with probability  $\epsilon \in [0, 1)$  whereas in the bad state each channel packet is lost with probability 1. Let  $\alpha$  and  $\beta$  denote the transition probabilities from the good state to the bad state and vice versa. Then, the average loss rate of the GE channel is given by  $\frac{\beta}{\alpha+\beta} \cdot \epsilon + \frac{\alpha}{\alpha+\beta}$ . As long as the channel stays in the bad state, the channel behaves as a burst erasure channel. In contrast, the channel behaves like an i.i.d. erasure channel when the channel stays in the good state. Consider the following *three-phase GE channel*: The simulation of the GE channel consists of three phases of equal duration, where  $\alpha$ ,  $\beta$  and  $\epsilon$  are fixed during the simulation except that  $\beta$  is set to one for the middle phase. In other words, there are no consecutive bad states in the middle phase, implying that the middle phase introduces fewer burst erasures than the other two phases.

For the three-phase GE channel with constant parameters  $(\alpha, \beta) = (0.01, 0.3)$ , we focus on the case  $T = 10$  and plot in Figures 4a and 4b the FLRs against the varying parameter  $\epsilon$  for the uncoded scheme, the network-adaptive streaming scheme, and the best non-adaptive (fixed-rate) streaming code  $\mathcal{C}_{T,B,N}$  whose coding rate does not exceed the average coding rate of the adaptive scheme. Their corresponding coding rates are plotted in Figure 4c, where the coding rate for the no-coding scheme is always one and thus omitted. Figures 4a, 4b and 4c show that compared to non-adaptive schemes, our adaptive scheme achieves significantly lower FLRs and significantly higher coding rates across all values of  $\epsilon$  between 0.01 and 0.1. For the case  $\epsilon = 0.04$  where the empirical distribution of burst lengths is shown in Figure 5, we show in Figure 6 the variation of average FLRs for our adaptive streaming scheme and UDP across the 360 sessions for  $\epsilon = 0.04$ . It can be seen from Figure 6 that our adaptive scheme achieves less than half of the no-coding loss rate for all sessions. In addition, we display the variation of the FEC redundancy (i.e., one minus coding rate) for our adaptive scheme in Figure 7, which demonstrates how quickly it reacts to erasures, especially at the transition between the first and middle phases and the transition between the middle and last phases.

The reason why our adaptive scheme significantly outperforms non-adaptive ones can be explained with the help of Figure 8. Suppose 11 out of 40 of the network packets are dropped as shown in Figure 8. Our adaptive coding scheme updates the code in this order:  $\mathcal{C}_{10,1,1}$  and  $\mathcal{C}_{10,5,2}$  before transmitting packets 4 and 18 respectively. Therefore, the subsequent five packets losses are all recovered by  $\mathcal{C}_{10,5,2}$  as shown in Figure 8, whereas the fixed-rate code  $\mathcal{C}_{10,4,4}$  can only recover one packet.

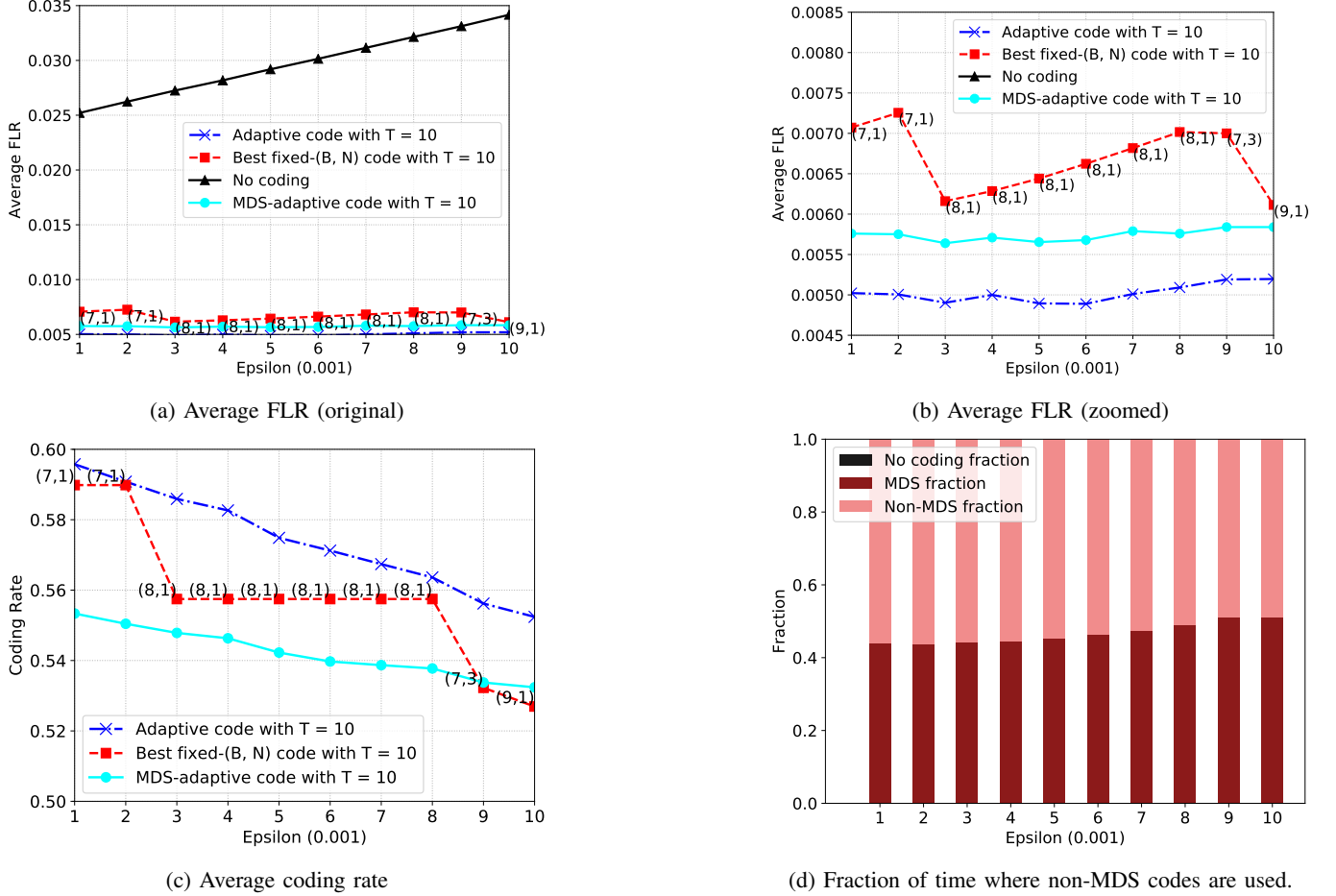


Fig. 4: Simulation results for different streaming schemes over the GE channel with  $(\alpha, \beta) = (0.01, 0.3)$

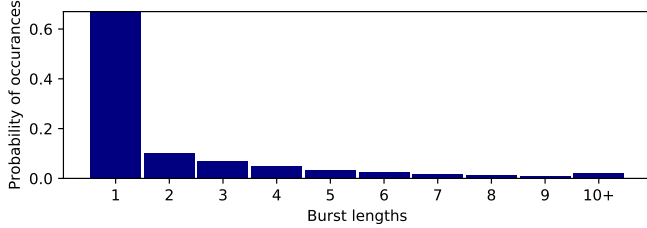


Fig. 5: Empirical burst-length distribution for  $\epsilon = 0.01$

2) *Simulated PESQ Scores*: In the previous subsection, we presented our simulation results in terms of FLRs for compressed multimedia frames where the duration and bit rate for each compressed frame are 10 ms and 240 kbit/s respectively. In this subsection, we would like to use the commonly adopted wideband PESQ (Perceptual Evaluation of Speech Quality) score [23] for uncompressed multimedia (WAV) files to demonstrate the advantage of using our network-adaptive streaming scheme over uncoded and non-adaptive streaming codes. To this end, we first choose a one-hour uncompressed speech file with sampling frequency of 16000 Hz and sample size of 16 bits and use the constant-bitrate (CBR) WMAv2 codec to generate compressed multimedia data with sampling frequency of 16000 Hz and bit rate of 240 kbit/s. Then, we use

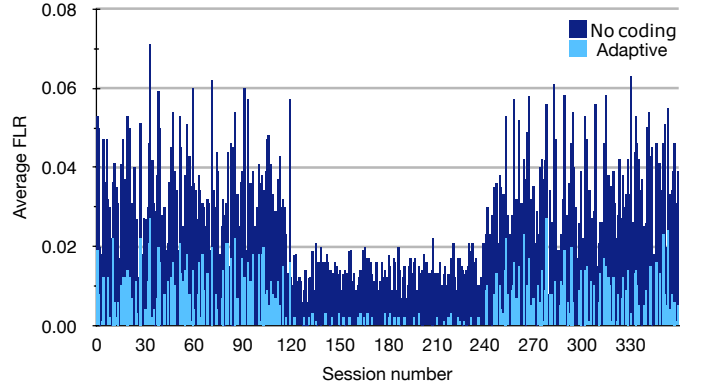


Fig. 6: Average FLRs for adaptive FEC over time for  $\epsilon = 0.04$

the network-adaptive, uncoded or best non-adaptive scheme to transmit the compressed multimedia through the three-phase GE channel as described in the previous subsection. Whenever a 300-byte compressed multimedia frame cannot be recovered by the destination, the lost frame is replaced with an 300-byte all-zero frame. The schematic diagram for the codec operations is shown in Figure 9.

For each 10-second session, a PESQ score is computed between the original uncompressed WAV audio and the recov-

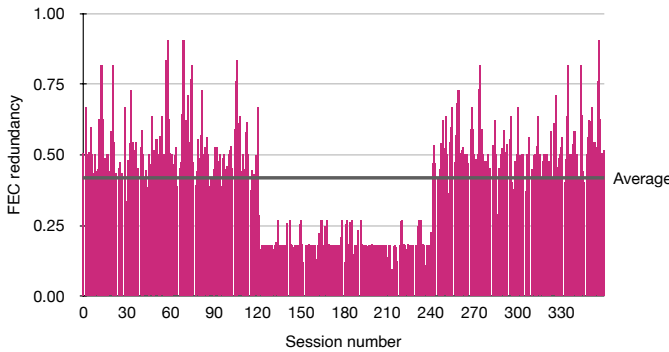


Fig. 7: FEC redundancy over time for  $\epsilon = 0.04$



Fig. 8: Packet losses recovered by different schemes

ered WAV audio for our network-adaptive streaming scheme. Each PESQ score ranges from 1 to 5 where a higher score means a better speech quality [23]. We plot in Figure 10 the simulated PESQ scores over  $M = 360$  sessions for our network-adaptive streaming scheme, the uncoded scheme and the best non-adaptive streaming code  $\mathcal{C}_{T,B,N}$  whose coding rate does not exceed the average coding rate of the network-adaptive scheme. We can see from 10 that our adaptive streaming scheme achieves a higher average PESQ score than uncoded and non-adaptive schemes.

We plot in Figure 12 the cumulative distribution function (cdf) of PESQ score (i.e., the fraction of the 360 sessions whose scores are less than a certain PESQ score) for each of the following schemes when  $\epsilon = 0.04$ : Our adaptive streaming scheme, the best non-adaptive streaming code and the uncoded scheme. It can be seen from Figure 12 that our adaptive scheme provides the best user experience compared to the uncoded and non-adaptive schemes. If the PESQ score of a session is lower than 3.6, many users will be dissatisfied by the unclear speech, and we will call such a session a *low-satisfaction* session. Figure 11 shows that our adaptive streaming scheme significantly reduces the fraction of low-satisfaction sessions compared to the uncoded and non-adaptive schemes.

**3) Optimal Streaming Codes vs. MDS-Based Streaming Codes:** In order to demonstrate the advantage of using our constructed streaming codes described in Section IV over traditional MDS-based codes, we consider the following *MDS-adaptive streaming scheme*: Instead of outputting the coding parameters  $(\hat{B}, \hat{N})$  for an optimal block code which corrects a length- $\hat{B}$  burst erasure and  $\hat{N}$  arbitrary erasures, the adaptive algorithm outputs a single coding parameter  $N$  of an MDS code which corrects only  $N$  arbitrary erasures such that the

resultant coding rate  $C(T, N, N) = \frac{T-N+1}{T+1}$  satisfies

$$C(T, N, N) \leq C(T, \hat{B}, \hat{N}) \leq C(T, N - 1, N - 1),$$

meaning that the resultant coding rate is the largest possible rate achieved by an MDS code that is less than  $C(T, \hat{B}, \hat{N})$  (cf. (1)). We plot in Figures 4a and 4b the FLRs achieved by the MDS-adaptive streaming scheme against  $\epsilon$  for the MDS-adaptive streaming scheme, and plot in Figure 4c their corresponding coding rates. Figures 4a, 4b and 4c show that compared to the MDS-adaptive scheme, our adaptive scheme achieves a considerably lower FLR and significantly higher coding rate across all values of  $\epsilon$  between 0.01 and 0.1. The superiority of our adaptive scheme to the MDS-adaptive scheme is due to the following fact displayed in Figure 4d: The fraction of non-MDS codes chosen by the adaptive algorithm used by our adaptive scheme is more than half for all  $\epsilon \in [0.01, 0.1]$ , implying that the optimal streaming codes chosen by our adaptive scheme are non-MDS over half of the time. Consequently, the streaming codes chosen by the MDS-adaptive streaming scheme are inferior to those chosen by our adaptive scheme over half of the time.

#### D. Experimental Results for a Wi-Fi Network

**1) Experimental Frame Loss Rates (FLRs):** In our real-world experiment, the source and the destination are connected to the same Wi-Fi network whose capacity is approximately 30 Mbit/s and the Wi-Fi network is subject to UDP cross traffic introduced by Iperf. We call the UDP cross traffic *offered load*, whose throughput is fixed at the beginning of the experiment and kept unchanged during the experiment. The average FLRs for our network-adaptive streaming scheme as described in Section VII-A and the uncoded scheme are plotted against the ratio of the offered load occupied by Iperf traffic in Figure 13a. In addition, we use the packet loss traces recorded during the real-world experiments performed for our adaptive streaming scheme to simulate the average FLR for the best non-adaptive (fixed-rate) streaming code  $\mathcal{C}_{T,B,N}$  whose coding rate does not exceed the average coding rate of the adaptive scheme. The average FLR for the best non-adaptive streaming code  $\mathcal{C}_{T,B,N}$  with parameters  $(B, N)$  is plotted in Figure 13a. Figure 13a and Figure 13c show that our adaptive streaming scheme achieves significantly lower average FLRs and higher average coding rate than the rest across most values of  $\epsilon$  between 0.01 and 0.1.

For interactive audio, low-fidelity sessions lead to unclear speech or even call termination which directly affects user experience. Figures 13b shows that our adaptive streaming scheme provides a substantially better audio quality than the other two.

For the case where the offered load equals 40% of the capacity, we display the empirical distribution of burst lengths in Figure 14 and show in Figure 15 the variation of average FLRs for our adaptive streaming scheme and UDP across the 360 sessions. It can be seen from Figure 15 that for more than 1/4 of the sessions that experience packet loss, our adaptive scheme achieves less than half of the no-coding loss rate. In addition, we display the variation of the FEC redundancy (i.e.,

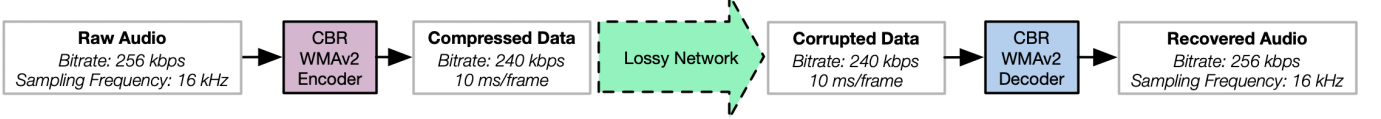


Fig. 9: Codec operations

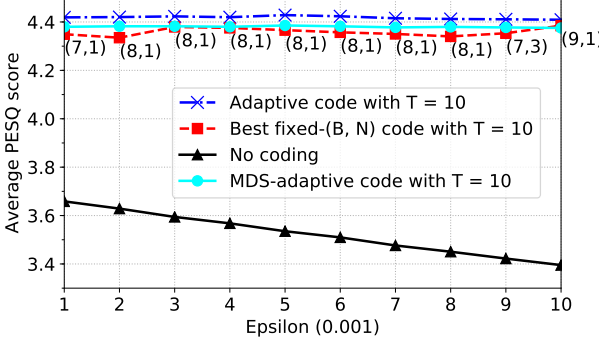


Fig. 10: Average PESQ score obtained from simulation (original and zoomed)

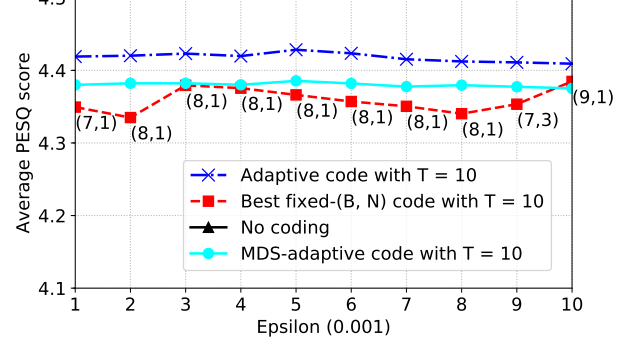


Fig. 10: Average PESQ score obtained from simulation (original and zoomed)

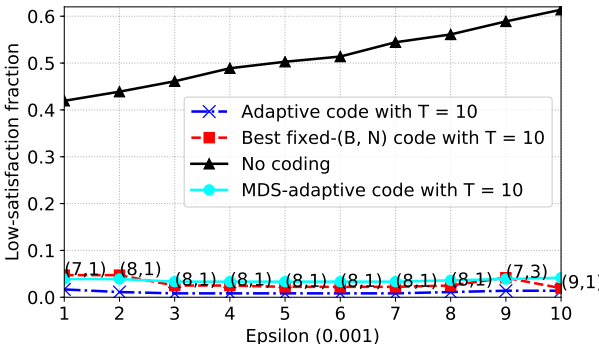


Fig. 11: Low-satisfaction fraction obtained from simulation (original and zoomed)

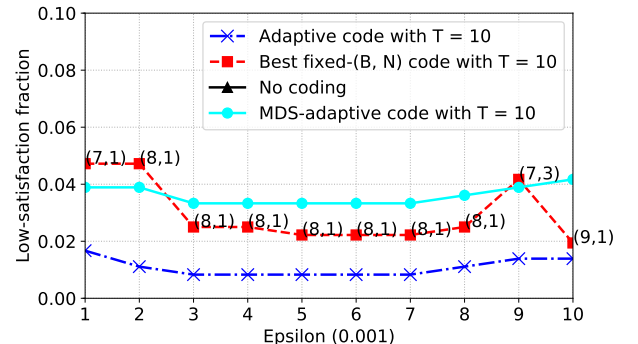
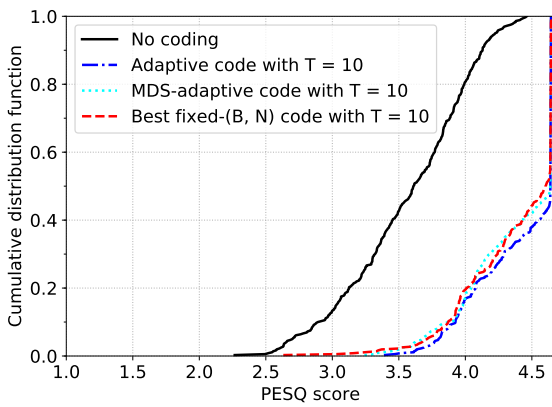


Fig. 11: Low-satisfaction fraction obtained from simulation (original and zoomed)

Fig. 12: The cdf of simulated PESQ score for adaptive FEC, MDS-adaptive FEC and non-adaptive FEC for  $\epsilon = 0.04$ 

one minus coding rate) for our adaptive scheme in Figure 16, which demonstrates how quickly it reacts to erasures.

2) *Experimental PESQ Scores:* In the previous subsection, we presented our experimental results in terms of FLRs for

compressed multimedia frames where the duration and bit rate for each compressed frame are 10 ms and 240 kbit/s respectively. In this subsection, we follow the audio and codec settings as described in Section VII-C2 (cf. Figure 9) and use the network-adaptive, uncoded or best non-adaptive scheme to transmit the compressed multimedia through the Wi-Fi network subject to Iperf UDP cross traffic as described in the previous subsection.

For each 10-second session, a PESQ score is computed between the original uncompressed WAV audio and the recovered WAV audio for our network-adaptive streaming scheme. The average PESQ scores over 360 sessions for our network-adaptive streaming scheme is plotted against the percentage of the network capacity occupied by Iperf traffic in Figure 17. In addition, we use the recorded packet loss traces to simulate the average PESQ scores for the uncoded scheme and the best non-adaptive streaming code  $\mathcal{C}_{T,B,N}$  whose coding rate does not exceed the average coding rate of the network-adaptive scheme. The average PESQ scores for the uncoded scheme and the best non-adaptive streaming code with parameters  $(B, N)$  are also plotted in Figure 17. We can see from 17 that our

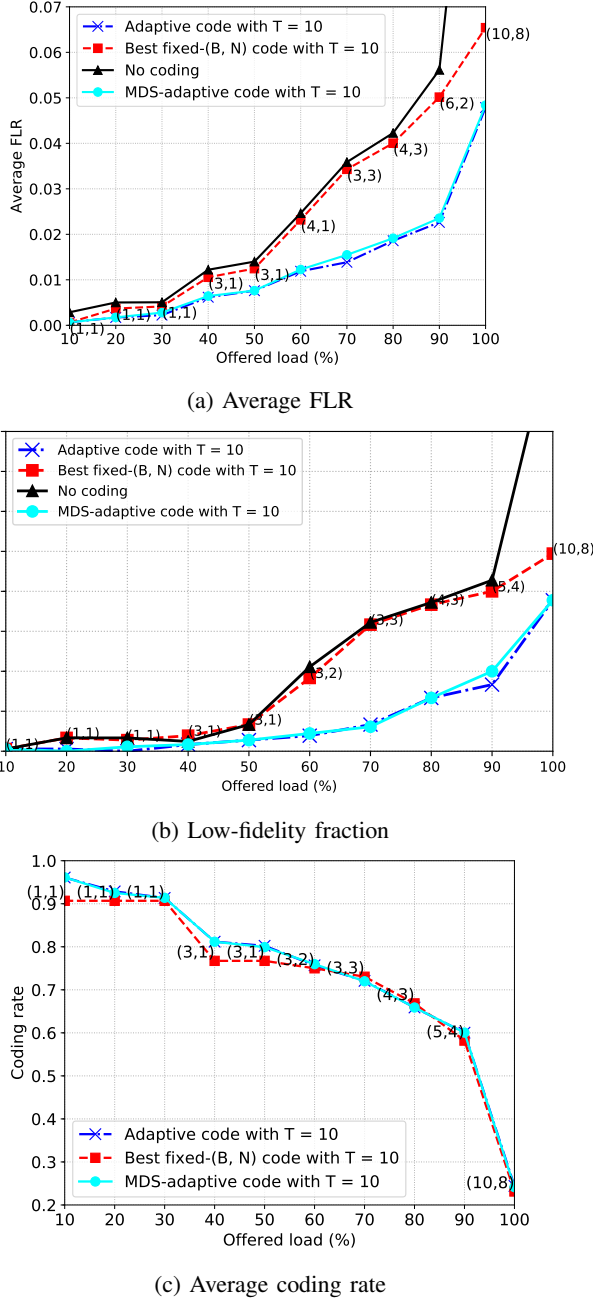


Fig. 13: Experimental results for different streaming schemes interfered by Iperf cross traffic

adaptive streaming scheme achieves a higher average PESQ score than uncoded and non-adaptive streaming schemes. In addition, Figure 18 shows that our adaptive streaming scheme significantly reduces the fraction of low-satisfaction sessions (with PESQ score lower than 3.6) compared to the uncoded and non-adaptive schemes.

We plot in Figure 19 the cdf of PESQ score (i.e., the fraction of the 360 sessions whose scores are less than a certain PESQ score) for each of the following schemes under 40%-capacity offered load: Our adaptive streaming scheme, the best non-adaptive streaming code and the uncoded scheme. It can be seen from Figure 19 that our adaptive scheme provides the best

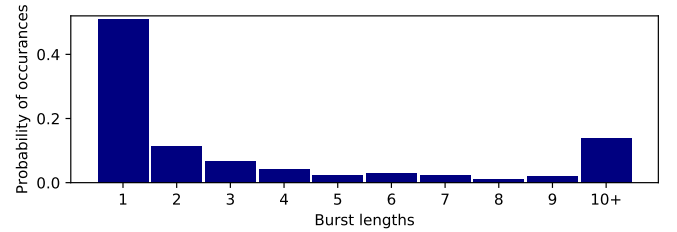


Fig. 14: Empirical burst-length distribution for 40%-capacity offered load

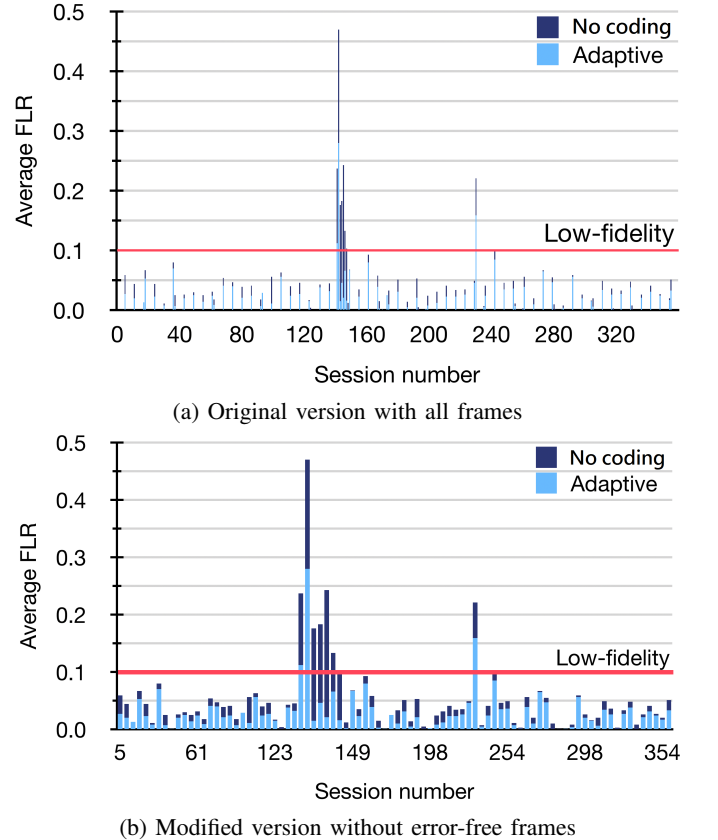


Fig. 15: Average FLRs for adaptive FEC over time for 40%-capacity offered load

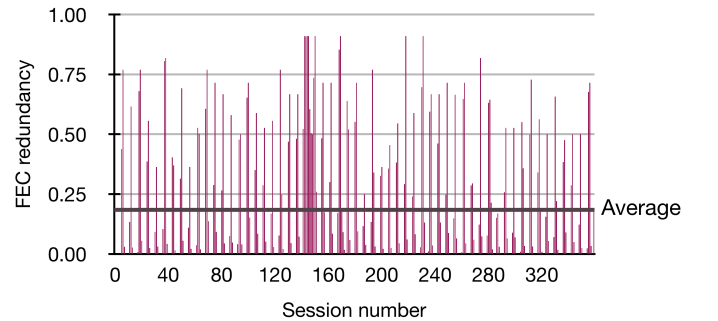


Fig. 16: FEC redundancy for 40%-capacity offered load

user experience compared to the uncoded and non-adaptive schemes.

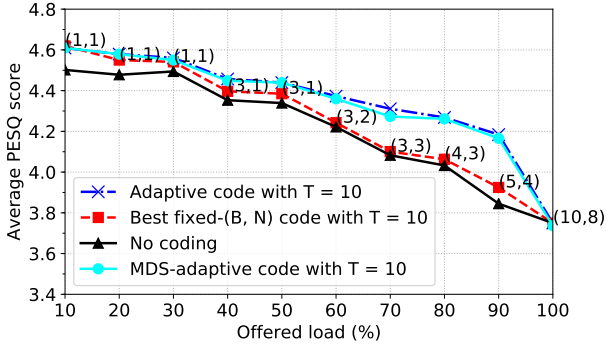


Fig. 17: Average PESQ score subject to Iperf traffic

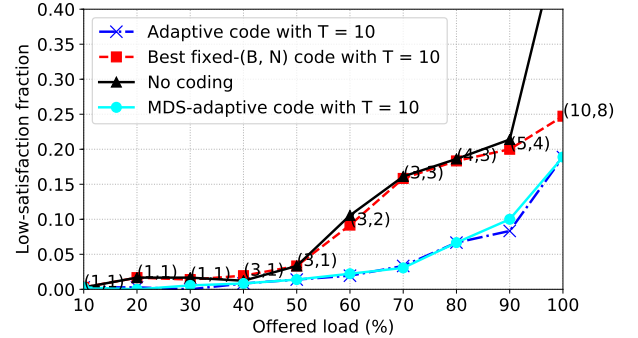


Fig. 18: Low-satisfaction fraction subject to Iperf traffic

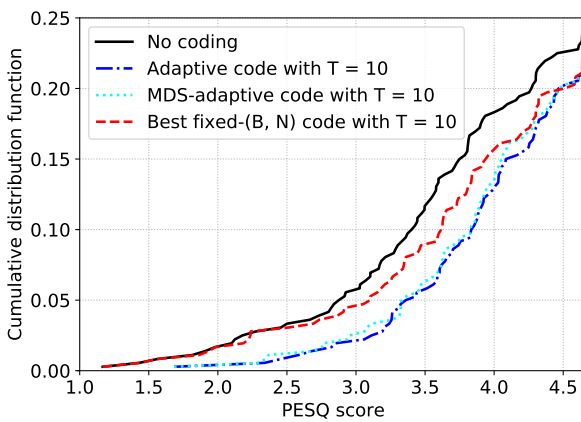


Fig. 19: The cdf of PESQ score for adaptive FEC, MDS-adaptive FEC and non-adaptive FEC for 40%-capacity offered load

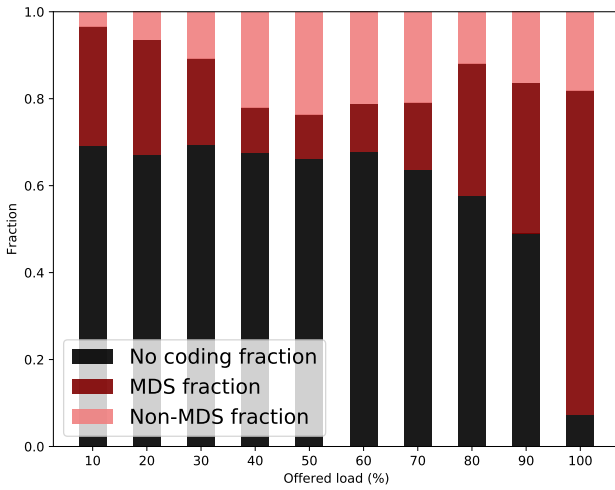


Fig. 20: Fraction of time where non-MDS codes are used.

3) *Optimal Streaming Codes vs. MDS-Based Streaming Codes:* We plot in Figures 13a, 13b, 17, 18 and 19 the respective average FLR, low-fidelity fraction, average PESQ score, low-satisfaction fraction and the PESQ cdf under 40%-capacity offered load for the MDS-adaptive streaming scheme as described in Section VII-C3, which show that our network-

strategy	FEC redundancy	average FLR	low-fi fraction
network-adaptive	19.03%	0.01190	0.03047
MDS-adaptive	20.17%	0.01757	0.03878
no coding	0%	0.03489	0.01856

(a)  $T = 10$ 

	16.6%	0.02586	0.07202
network-adaptive	17.2%	0.02617	0.07756
no coding	0%	0.04003	0.17452

(b)  $T = 9$ 

	16.10%	0.00486	0.00831
network-adaptive	17.24%	0.01040	0.01108
no coding	0%	0.02486	0.13573

(c)  $T = 11$ 

TABLE II: Performance of different streaming strategies for 30%-capacity offered load

adaptive scheme is marginally better than the MDS-adaptive scheme. This can be explained by Figure 20 which shows that the fraction of non-MDS codes chosen by the adaptive algorithm used by our adaptive scheme is less than 25% for all  $\epsilon \in [0.01, 0.1]$ , implying that the optimal streaming codes chosen by our adaptive scheme are non-MDS less than 25% of the time.

Since it is unclear from viewing Figures 13a, 13b, 17 and 18 that our network-adaptive streaming scheme can significantly outperform the MDS-adaptive streaming scheme in real-world networks, we use the recorded packet loss traces obtained from a repeated experiment with 30%-capacity offered load to compare the network-adaptive streaming scheme with the MDS-adaptive streaming scheme for  $T = 10$ . Table IIa shows that although the two schemes have similar rates, the network-adaptive streaming scheme achieves around 80% of the average FLR and 80% of the low-fidelity sessions achieved by the MDS-adaptive streaming scheme, which implies that our constructed optimal streaming codes outperforms traditional MDS-based streaming codes in real-world networks. The reduction in FLR is not surprising because our optimal streaming codes treat burst erasures and arbitrary erasures differently while MDS-based codes do not differentiate them. Even if  $T$  slightly deviates from 10, our experimental results displayed in Tables IIb and IIc show that the network-adaptive streaming scheme compared with the MDS-adaptive streaming scheme

can achieve a considerable reduction in FLR. In particular, for  $T = 11$ , although the two adaptive schemes have similar rates, the network-adaptive streaming scheme achieves around 50% of the average FLR and 75% of the low-fidelity sessions achieved by the MDS-adaptive streaming scheme.

### VIII. CONCLUSION AND FUTURE WORK

We have designed a network-adaptive FEC streaming scheme which consists of (i) a network-adaptive algorithm for estimating the coding parameters of streaming codes that correct both burst and arbitrary network packet losses, and (ii) an explicit construction of low-latency optimal streaming codes over GF(256) for  $T \leq 11$ . The computation bottleneck of our network-adaptive streaming scheme is bounded above by  $O(T^3)$  complexity, where the bottleneck upper bound is due to the complexity of decoding a length- $(T + 1)$  block code using Gauss-Jordan elimination [32]. More precisely, the computation bottleneck is close to  $O(D^3)$  where  $D$  denotes the average number of lost packets in a sliding window of size  $T + 1$ , where the bottleneck is due to the average complexity of decoding the lost packets in a sliding window of size  $T + 1$ . Real-world experiments reveal that our adaptive streaming scheme significantly outperforms non-adaptive ones in terms of FLRs and PESQ scores. There are several interesting directions for future investigation: (i) Finding the largest  $T$  such that optimal streaming codes exist over GF(256) remains open. (ii) Future work may explore the interplay between our adaptive streaming scheme which adjusts the coding rate in real time and existing congestion control algorithms that adjust the sizes of streaming messages in real time. (iii) The investigation of how multiple instances of our network-adaptive scheme compete with each other in a congested environment is interesting. (iv) The choice of  $L$  for our heuristic adaptive algorithm, set to 1000 in this work, could be optimized with extra effort. Also, machine learning techniques could be used to develop new network-adaptive algorithms. (v) This work compares FEC schemes only. Considering additional complementary methods in existing industrial schemes (e.g., Skype, WebRTC and other ARQ-based schemes) such as Adaptive Media Playout, adaptive live encoder and retransmissions is meaningful.

### REFERENCES

- [1] International Telecommunication Union, “One-way transmission time,” Recommendation G.114, May 2003.
- [2] T. Stockhammer and M. Hannuksela, “H.264/AVC video for wireless transmission,” *IEEE Wireless Commun.*, vol. 12, pp. 6 – 13, Aug. 2005.
- [3] A. Badr, A. Khisti, W.-T. Tan, and J. Apostolopoulos, “Perfecting protection for interactive multimedia: A survey of forward error correction for low-delay interactive applications,” *IEEE Signal Process. Mag.*, vol. 34, pp. 95 – 113, 2017.
- [4] R. G. Gallagher, “Low density parity check codes,” *IRE Transactions on Inf. Theory*, vol. IT-8, pp. 21 – 28, 1962.
- [5] D. J. C. MacKay and R. M. Neal, “Near Shannon limit performance of low density parity check codes,” *Electronics Letters*, vol. 33, no. 6, pp. 457 – 458, 1997.
- [6] M. Luby, “LT codes,” in *Proc. Annu. IEEE Symp. Foundations Computer Science*, Vancouver, BC, Canada, Nov. 2002.
- [7] A. Shokrollahi, “Raptor codes,” *IEEE Trans. Inf. Theory*, vol. 52, no. 6, pp. 2551 – 2567, 2006.
- [8] European Telecommunications Standards Institute, “Digital video broadcasting (DVB); Second generation framing structure, channel coding and modulation systems for broadcasting, interactive services, news gathering and other broadband satellite applications; Part 1: DVB-S2,” ETSI EN 302 307-1, Nov. 2014.
- [9] ———, “Digital video broadcasting (DVB); Transport of MPEG-2 TS based DVB services over IP based networks,” ETSI TS 102 034, Apr. 2016.
- [10] J. Korhonen and P. Frossard, “Flexible forward error correction codes with application to partial media data recovery,” *Signal Processing: Image Communication*, vol. 24, no. 3, pp. 229 – 242, 2009.
- [11] J. Wang and D. Katabi, “ChitChat: Making video chat robust to packet loss,” Tech. Rep.
- [12] M. Nagy, V. Singh, J. Ott, and L. Eggert, “Congestion control using FEC for conversational multimedia communication,” in *Proc. the 5th ACM Multimedia Systems Conference*, Singapore, Mar. 2014, pp. 191 – 202.
- [13] S. Holmer, M. Shemer, and M. Paniconi, “Handling packet loss in WebRTC,” in *Proc. IEEE Intl. Conference on Image Process.*, Melbourne, VIC, Australia, Sep. 2013.
- [14] T. Huang, P. Huang, K. Chen, and P. Wang, “Could Skype be more satisfying? A QoE-centric study of the FEC mechanism in an Internet-scale VoIP system,” *IEEE Netw.*, vol. 24, no. 2, pp. 42 – 48, 2010.
- [15] E. Martinian and C.-E. W. Sundberg, “Burst erasure correction codes with low decoding delay,” *IEEE Trans. Inf. Theory*, vol. 50, no. 10, pp. 2494 – 2502, 2004.
- [16] S. L. Fong, A. Khisti, B. Li, W.-T. Tan, X. Zhu, and J. Apostolopoulos, “Optimal streaming codes for channels with burst and arbitrary erasures,” *IEEE Trans. Inf. Theory*, vol. 15, no. 7, pp. 4274 – 4292, 2019.
- [17] M. N. Krishnan and P. V. Kumar, “Rate-optimal streaming codes for channels with bursts and isolated erasures,” in *Proc. IEEE Intl. Symp. on Inf. Theory*, Vail, CO, USA, Jun. 2018, pp. 1809 – 1813.
- [18] G. Joshi, Y. Kochman, and G. W. Wornell, “On playback delay in streaming communication,” in *Proc. IEEE Intl. Symp. on Inf. Theory*, Cambridge, MA, USA, Jul. 2012, pp. 2856 – 2860.
- [19] G. Joshi, Y. Kochman, and G. W. Wornell, “The effect of block-wise feedback on the throughput-delay tradeoff in streaming,” in *Proc. IEEE Conf. Computer Commun. Workshops (INFOCOM Workshops)*, Toronto, ON, Canada, Apr. 2012, pp. 227 – 232.
- [20] D. Malak, M. Médard, and E. M. Yeh, “Tiny codes for guaranteeable delay,” *arXiv*, Feb. 2019, arXiv:1806.05776 [cs.IT].
- [21] A. Cohen, D. Malak, V. B. Bracha, and M. Médard, “Adaptive causal network coding with feedback for delay and throughput guarantees,” *arXiv*, May 2019, arXiv:1905.02870 [cs.IT].
- [22] S. L. Fong, S. Emara, B. Li, A. Khisti, W.-T. Tan, X. Zhu, and J. Apostolopoulos, “Low-latency network-adaptive error control for interactive streaming,” in *To be presented at 27th ACM International Conference on Multimedia*, Nice, France, Oct. 2019.
- [23] International Telecommunication Union, “Wideband extension to recommendation p.862 for the assessment of wideband telephone networks and speech codecs,” Recommendation P.862.2, Nov. 2007.
- [24] F. J. MacWilliams and N. J. A. Sloane, *The Theory of Error-Correcting Codes*, 1st ed. Amsterdam, Holland: North-Holland, Netherlands, 1988.
- [25] G. D. Forney, “Burst-correcting codes for the classic bursty channel,” *IEEE Trans. Inf. Theory*, vol. 19, no. 5, pp. 772 – 781, 1971.
- [26] J. Valin, K. Vos, and T. Terriberry, “Definition of the opus audio codec,” Internet Requests for Comments, RFC Editor, RFC 6716, Sep. 2012. [Online]. Available: <https://tools.ietf.org/html/rfc6716>
- [27] International Telecommunication Union, “Pulse code modulation (PCM) of voice frequencies,” Recommendation G.711, Nov. 1998.
- [28] E. N. Gilbert, “Capacity of a burst-noise channel,” *Bell System Technical Journal*, vol. 39, pp. 1253–1265, Sep. 1960.
- [29] E. O. Elliott, “Estimates of error rates for codes on burst-noise channels,” *Bell System Technical Journal*, vol. 42, pp. 1977 – 1997, Sep. 1963.
- [30] G. Hasslinger and O. Hohlfeld, “The Gilbert-Elliott model for packet loss in real time services on the Internet,” in *14th GI/ITG Conference – Measuring, Modelling and Evaluation of Computer and Communication Systems (MMB)*, Dortmund, Germany, Mar./Apr. 2008.
- [31] O. Hohlfeld, R. Geib, and G. Hasslinger, “Packet loss in real-time services: Markovian models generating QoE impairments,” in *16th International Workshop on Quality of Service*, Enschede, Netherlands, Jun. 2008.
- [32] R. W. Farebrother, *Linear Least Squares Computations*. New York, NY, USA: Marcel Dekker, Inc., 1988.